Distonic radical anion species in cysteine oxidation cycle

Journal:	*Physical Chemistry Chemical Physics*
Manuscript ID	CP-ART-04-2020-002165.R1
Article Type:	Paper
Date Submitted by the Author:	14-Apr-2020
Complete List of Authors:	Qin, Zhengbo; Anhui Province Key Laboratory of Optoelectric Materials Science and Technology, Anhui Normal University Hou, Gao-Lei; KU Leuven, Department of Physics and Astronomy Yang, Zheng; Pacific Northwest National Laboratory Valiev, Marat; Pacific Northwest National Laboratory Wang, Xue-Bin; Pacific Northwest National Laboratory

PAPER

Received 00th January 20xx,
Accepted 00th January 20xx

DOI: 10.1039/x0xx00000x

www.rsc.org/chemicalscience

Distonic radical anion species in cysteine oxidation processes†

Zhengbo Qin,*[a] Gao-Lei Hou,[b] Zheng Yang,[b] Marat Valiev,*[c] and Xue-Bin Wang*[b]

Oxidation of cysteine residues constitutes an important regulatory mechanism in the function of biological systems. Much of this behavior is controlled by the specific chemical properties of the thiol side-chain group, where reactions with reactive oxygen species take place. Herein, we investigated the entire cysteine oxidation cycle Cys-SH → Cys-SO_nH (n = 1, 2, 3) using cryogenic negative ion photoelectron spectroscopy and quantum-chemical calculations. The conventional view on the first reversible oxidation step (n = 1) is associated with sulfenate species. Yet our results indicate that an alternative option exists in the form of novel distonic radical anion •OS-$CH_2CH(NH_2)$-COO^- with an unpaired electron on the thiol group and excess negative charge on the carboxylate. Higher order oxidation states (n = 2, 3) are thought to be associated with irreversible oxidative damage, and our results show that excess negative charge in those cases migrates to -SO_n^- group. Furthermore, these species are stable towards *1e* oxidation, as opposed to the n = 1 case that undergoes intra-molecular proton transfer. The molecular level insights reported in this work provide direct spectroscopic evidences towards unique chemical versatility of Cys-sulfenic acid (Cys-SOH) in post-translational modifications of protein systems.

1. Introduction

Cysteine is one of the only two standard amino acids with sulfur containing side chains. It is closely related to serine, having thiol (-SH) instead of hydroxyl (-OH) group. While both oxygen and sulfur belong to the same family in the periodic table, the sulfur is less electronegative and can adopt wide range of oxidation states.[1] All this makes cysteine thiol group much more amenable to the attack by reactive oxygen species (ROS), forming the basis for post-translational modifications of protein systems[2] and making it an important enzymatic redox sensor.[3,4] The oxidative modification of cysteine consists of several stages.[5,6] The first reversible step involves of formation of sulfenic acid R–SOH.[7] The latter species are highly reactive and can be further oxidized to more stable sulfinic (R–SO_2H) and further to sulfonic (R–SO_3H) acids (Scheme 1). The transition to these much higher oxidation state species is usually regarded as irreversible, which is considered to be associated with the oxidative damage.[5,8] Overall cysteine oxidation is also an integral part of disulfide formation, which is regarded as one of main reversible reaction pathways.[9,10]

Ultimately the fate of the cysteine residue in the protein depends on number of factors, e.g. local environment, access to ROS species, etc. Underlying all of them are the intrinsic chemical properties of thiol group. The latter can be most appropriately characterized in the absence of protein matrix under gas phase or cluster conditions. The importance of such investigations has been amply demonstrated in a number of recent studies.[11-14] The irreversible reaction process for the cysteine sulfonate anion and its oxidation have been studied through mass spectrometry and infrared multiple photon dissociation spectroscopy (IRMPD).[15-18] The present work continues these efforts by extending spectroscopic characterization onto the entire cysteine oxidation products by means of cryogenic negative ion photoelectron spectroscopy (cryo-NIPES) which was coupled with electrospray ionization source (ESI). The key advantages of ESI-NIPES are that (1) solution-phase anionic species including reactive transient radical anions can be isolated and transported into the gas phase,[19,20] and (2) the electronic structures and geometries of both anions and 1e detached (oxidized) neutrals can be directly probed, affording rare opportunity to study electron detachment induced proton or hydrogen atom transfers in well-defined systems.[21]

2. Experimental method

The experiments were carried out using a size-selected cryogenic NIPES instrument coupled with an ESI source.[22] Oxidized cysteine products were produced by spraying a 0.1 mM solution of the cysteine in water/methanol (1/3) solvent at pH = 8-9 in the presence of diluted O_3 produced via a lab-made ozone generator. These oxidized cysteine products were then subjected to mass-selected cryo-NIPES measurements.

---

[a] *Anhui Province Key Laboratory of Optoelectric Materials Science and Technology, Anhui Normal University, Wuhu, 241000, China. E-mail: wave0403@163.com.*
[b] *Physical Sciences Division, Pacific Northwest National Laboratory, 902 Battelle Boulevard, P. O. Box 999, MS K8-88, Richland, Washington 99352, USA. E-mail: xuebin.wang@pnnl.gov.*
[c] *Environmental Molecular Sciences Laboratory, Pacific Northwest National Laboratory, P. O. Box 999, Richland, WA 99352, USA. E-mail: marat.valiev@pnnl.gov.*

† Footnotes relating to the title and/or authors should appear here.
† Electronic Supplementary Information (ESI) available. See DOI: 10.1039/x0xx00000x

3. Computational methodology

All theoretical calculations were performed using the Gaussian 09 package.[23] Structure optimization and frequency calculations were performed at the level of CAM-B3LYP[24]/maug-cc-pVTZ[25] for all species. For isomers of sulfenyl radical anion (2A) the energies of the CAM-B3LYP optimized structures were reevaluated at the coupled cluster single-double and perturbative triple CCSD(T)[26]/maug-cc-pVTZ level. The excited state energies were obtained by TD-DFT[27,28] using the CAM-B3LYP functional with the maug-cc-pVDZ basis set.[25] Natural population analysis (NPA)[29] was performed at the level of CAM-B3LYP/maug-cc-pVTZ theory. Further experimental and theoretical details can be found in supporting information.

4. Results and discussion

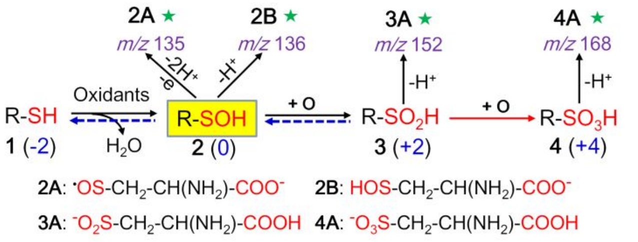

Scheme 1 Scheme of the cysteine oxidation to the sulfenic (**2**), sulfinic (**3**), and sulfonic (**4**) acids in the presence of oxidants. Green star represents experimentally observed species via NIPES experiments; blue numbers in the bracket denotes nominal oxidation state of sulfur.

One of the main highlights of this investigation is the detection of new type of oxidized cysteine species - sulfenyl radical anion (**2A**, see Scheme 1). It may be formed most straightforwardly by double deprotonation of cysteine-sulfenic acid under basic conditions, followed by one electron autodetachment of [$^{-}$OS-CH$_2$CH(NH$_2$)-COO^{-}] during the ESI process. Similar processes have been employed previously to generate gaseous radical anions.[30-33] The resulting **2A** species are what are known as distonic anion radicals, and characterized by separation between spin (radical electron on thiol group) and negative charge density (on carboxylate group). What makes these types of molecules so interesting, is that the properties of the radical center are a sensitive function of charge region, which provides a potential mechanism of controlling the overall reactivity.[34,35]

The spectrum for newly observed radical anion species **2A** (*m/z*=135) is shown in Fig. 1a. There are several tautomer possibilities for **2A** — sulfenyl radical with deprotonated carboxylic group (**2A$_0$**, Fig. 2), α-carbon radical with protonated sulfenic group (**2A$_1$**, Fig. S1), and α-carbon radical with protonated carboxylate group (**2A$_2$**, Fig. S1). *Ab initio* calculations at the CCSD(T) level of theory indicate that, among these three choices, the sulfinyl radical, **2A$_0$**, has the lowest energy. The energies of **2A$_1$** and **2A$_2$** are much higher, 13.80 and 19.40 kcal/mol above **2A$_0$** respectively. In addition to having the lowest energy, the **2A$_0$** tautomer also shows the best agreement with respect to vertical detachment energy (VDE). For transition to singlet state we calculated VDE of 4.62 eV compared to the experimental value of 4.61 eV (Table 1 and S1). For transition to a triplet state, the calculated value is 4.47 eV, again compared excellently with 4.46 eV experimental value. Observation and identification of these two states in the spectrum is unambiguously verified by Franck-Condon simulations (Fig. S5). Furthermore, for **2A$_0$**, we observe good agreement between the overall simulated (density-of-states (DOS) and TDDFT) and the experimental spectrum (Fig. S6-S7). In contrast, the VDE values and simulated spectrum based on **2A$_1$** and **2A$_2$** are very different from the experiments (Table S1, Fig. S6-S7). Close examination of the **2A** spectrum reveals a very weak between 2-4 eV electron binding energy (EBE) band (Fig. 1a). Its intensity appears to be dependent on the mixing time of the spraying solution assigned to the formation of dimerized dianion [CyS(=O)$_2$SCy]$^{2-}$ with the same m/z = 135 as 2A (see Fig. S8) as suggested in a previous mass spectrometric study.[15]

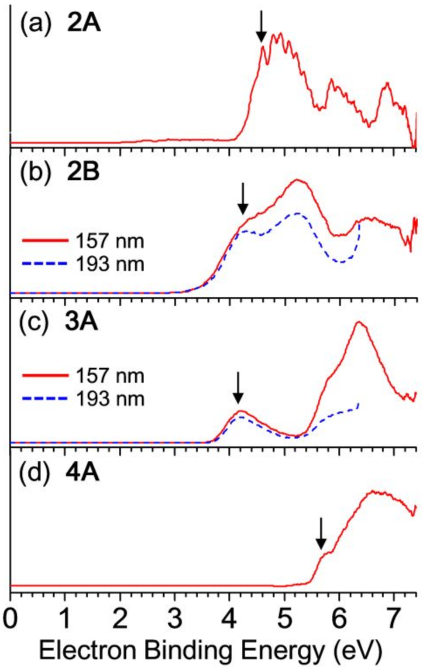

Fig. 1 The 20 K NIPE spectra (red curves) of the cysteine-sulfenic acid derived radical anion (**2A**) (a), cysteine sulfenate (**2B**) (b), sulfinate (**3A**) (c), and sulfonate anions (**4A**) (d). Black arrows indicate the experimentally measured VDEs.

Molecular orbital (MO) analysis of **2A$_0$** indicates that unpaired electron, or the singly occupied molecular orbital (SOMO), resides on the -SO moiety (Fig. S15 and S19). At the same time the majority of excess negative charge concentrates on the carboxylate, which confirms distonic nature of the species. One of the characteristic features of distonic radical anions that have been discussed at great length[34-37] is the so-called SOMO-HOMO energy inversion, i.e. when SOMO is no longer the highest energy orbital. The same phenomenon was observed for **$2A_0$** as well, i.e. the SOMO located slightly lower (~2.8 kcal/mol) than the HOMO orbital associated on the carboxylic group. In the light of these observations, one would almost expect that the electron detachment should occur primarily off the carboxylate group. Yet the charge analysis of the configuration right after the detachment clearly indicates the electron is ejected from neutral radical -SO group, indicating that this is the most reactive part of the molecule. As a result of this, -SO acquires excess positive charge (see Fig. 3), which is then neutralized by negative carboxylate by relaxing into five-membered ring structure (**$2A_0$'**). It results in significant structural transformation, which is corroborated by the broad nature of the spectrum.

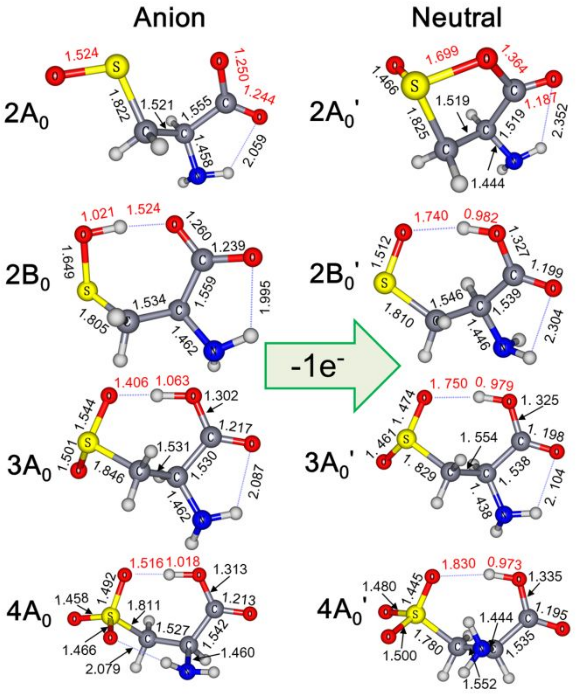

Fig. 2 The most stable optimized structures of the cysteine-sulfenic acid derived radical anion (**$2A_0$**), cysteine sulfenate (**$2B_0$**), sulfinate (**$3A_0$**), and sulfonate anion (**$4A_0$**) and their corresponding photo-detached neutral counterparts. Selective bond distances in Å are shown.

Table 1 Experimental and calculated ADEs and VDEs of the species **$2A_0$-$4A_0$** and **$2B_0$**. The numbers in the parentheses indicate the experimental uncertainties. All energies are in eV.

Species	ADE		VDE	
	Calc.	Exp.	Calc.	Exp.
$2A_0$ (singlet)	1.80	—	4.62	4.61(8)
$2A_0$ (triplet)	4.10	4.14(6)	4.47	4.46(10)
$2B_0$	2.71	3.02(8)	4.31	4.27(5)
$3A_0$	3.71	3.69(7)	4.25	4.21(6)
$4A_0$	5.52	5.42(6)	5.73	5.71(6)

One can argue that the destabilization or higher energy of the HOMO orbital in **$2A_0$** can be readily understood as a result of Coulomb repulsion that such orbital experiences on the negatively charged carboxylate group. Subsequently, one of the mechanisms by which the normal MO order can be restored consists of protonation of the carboxylate group, i.e. pH-induced MO conversion.[34] In the case of **$2A_0$**, such pH-induced conversion leads naturally to well-known sulfenate species (more precisely a neutral form of thereof), which are known to play an important role in reversible oxidation of cysteine residues.[5-7]

The sulfenate species (m/z=136) were indeed readily detected in our experiment. The resulting spectrum is shown on Fig. 1b. Calculations show that the lowest energy isomer (**$2B_0$**, see Fig. 2 and Fig. S2) features protonated sulfenyl group, which is expected given that it is a much weaker acid (pK_a ~ 8) compared to carboxylic group (pK_a ~ 4.8).[39] Further support for **$2B_0$** comes from the fact its calculated VDE value of 4.31 eV is in good agreement with experimental estimate of 4.27 eV. Charge analysis (see Fig. 3) indicates that, similar to **$2A_0$**, the electron detachment takes place from now protonated -SOH group. However, the mechanism for neutralizing the resulting positive charge on -SOH group is different. It can be readily accomplished by proton transfer (PT) back to negatively charged carboxylate group, which brings us to protonated form of distonic radical anion **$2A_0$**. This PT behavior is consistent with the broad nature of the spectrum of **$2B_0$**, which indicates substantial structural rearrangement during electron detachment.

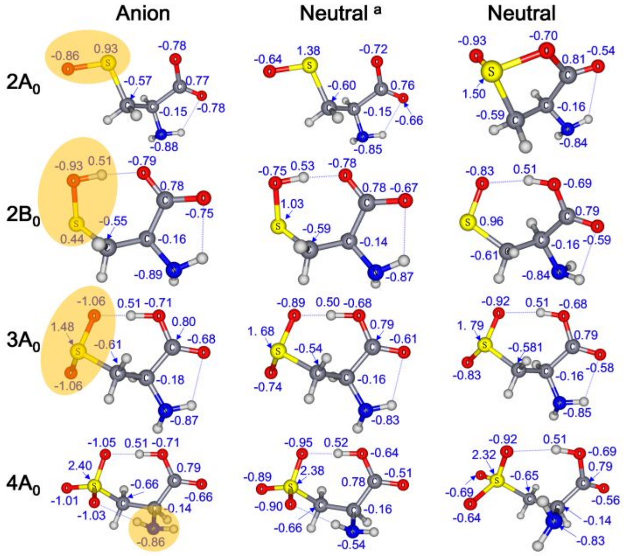

Fig. 3 The NPA charges on C, N, O and S atoms and H atom in O-H⋯O hydrogen bond (blue) for the most stable structures of **$2A_0$**, **$2B_0$**, **$3A_0$** and **$4A_0$** and their neutral counterparts. ([a]NPA charges on these atoms for the neutrals at anion's geometry).

As with previous investigations,[15] we have also detected higher order oxidation products — cysteine sulfinate **3A** (*m/z* = 152), and sulfonate **4A** (*m/z* = 168) anions. One important characteristic feature of higher oxidized states of cysteine is the increased acidity of -SO_n group ($pK_a \leq 2$). Consequently, *ab-initio* calculation shows the most stable configurations of both species, **3A**$_0$ and **4A**$_0$, (see Fig. 2), feature protonated carboxylate group. As shown on Table 1, the VDE values for these conformers are also in good agreement with experimental estimates. Similar to sulfenic species, the carboxylic group in lowest energy sulfinate structure (**3A**$_0$) forms intra-molecular hydrogen bonds to both -SO_2 and -NH_2 groups. Charge analysis indicates that similar to **2A**$_0$ and **2B**$_0$, the electron detachment in **3A**$_0$ again occurs from sulfur side of the molecule. Since the latter (-SO_2), now carries a negative charge, after electron detachment the system ends up in essentially neutral configuration and, in contrast to **2A**$_\mathbf{0}$ and **2B**$_\mathbf{0}$, only minor changes to the structure are required to accommodate new state.

In the case of sulfonate (**4A**$_0$), the intra-molecular hydrogen bond between carboxylic and amino group disappears, and amino group instead makes contact with -SO_3 group. The latter interaction becomes even more pronounced in the neutral state. The reason for this behavior becomes clear from charge analysis, which indicates that, unlike all previous cases, electron detachment of cysteine sulfonate occurs off the -NH_2 group (Fig. 3). This explains unusually high increase in electron binding energy in sulfonate species.

The results of combined cryo-NIPES and *ab-initio* analysis provide several important insights into oxidation chemistry of cysteine. The detection of new distonic radical anion species in gas phase conditions raises the possibility that such oxidized intermediates may also play a role in cysteine redox chemistry in biological systems. The stability of such species[33] is hinged upon the presence of negative charge region that can stabilize the radical center (-$SO^\bullet$). Should such situation be realized the distonic radical species may provide another potential mechanism of regulating oxidative response via specific electric field effects in the local protein environment.[40,41]

Conclusions

Contrary to the view that the first reversible oxidation step is associated with sulfinate species, a novel distonic radical anion $\bullet OS\text{-}CH_2CH(NH_2)\text{-}COO^-$ has been identified from direct cryo-NIPES experiments with inverted SOMO-HOMO energy order that can be restored via protonation.

In terms of the overall oxidation cycle, the distonic species can be thought of as precursor to cysteine sulfenic acid, generating the latter as a result of *1e,* H^+ addition. This implies that distonic radical anion, alongside sulfenic acid, may participate in *reversible* cysteine oxidation processes.

Conflicts of interest

The authors declare no competing financial interest.

Acknowledgements

This research was supported by the U.S. Department of Energy (DOE), Office of Science, Office of Basic Energy Sciences, Division of Chemical Sciences, Geosciences and Biosciences (X.-B.W. and M. V.) and was performed at the EMSL, a national scientific user facility sponsored by DOE's Office of Biological and Environmental Research and located at Pacific Northwest National Laboratory. Z. B. Q. thank additional supports from the National Science Foundation of China (Grant Nos. 21873003 and 21503003), and Special Program for Applied Research on Super Computation of the NSFC-Guangdong Joint Fund (the second phase) (Grant No. U1501501) and Super Computation of Shenzhen.

References

1 K. G. Reddie, K. S.Carroll, Current opinion in chemical biology, 2008, **12**, 746.
2 C. E. Paulsen, K. S. Carroll, Chem. Rev., 2013, **113**, 4633.
3 V. Gupta, K. S. Carroll, Biochim Biophys Acta, 2014, **1840**, 847-875.
4 C. Jacob, A. L. Holme, F. H. Fry, Org. Biomol. Chem. 2004, **2**, 1953-1956.
5 M. K. Lo Conte, S. Carroll, J. Biol. Chem., 2013, **288**, 26480.
6 C. Waszczak, S. Akter, S. Jacques, J. Huang, J. Messens, F. Van Breusegem, J. Exp. Bot., 2015, **66**, 2923.
7 A. Claiborne, H. Miller, D. Parsonage, R. P. Ross, FASEB J., 1993, **7**, 1483.
8 G. Roos, J. Messens, Free radical biology & medicine, 2011, **51**, 314.
9 C. C. Winterbourn and M. B. Hampton, Free Radical Bio. Med., 2008, **45**, 549.
10 M. Gongora-Benitez, J. Tulla-Puche and F. Albericio, Chem. Rev., 2014, **114**, 901.
11 E. V. Beletskiy, J. Schmidt, X.-B. Wang, S. R. Kass, J. Am. Chem. Soc., 2012, **134**, 18534.
12 A. Shokri, J. Schmidt, X.-B. Wang, S. R. Kass, J. Am. Chem. Soc., 2012, **134**, 2094.
13 S. H. M. Deng, X.-Y. Kong, Zhang, G. Y. Yang, W.-J. Zheng, Z.-R. Sun, D.-Q. Zhang, X.-B. Wang, J. Phys. Chem. Lett., 2014, **5**, 2155.
14 K. Bhaskaran-Nair, M. Valiev, S. H. M. Deng, W. A. Shelton, K. Kowalski, X.-B. Wang, J. Chem. Phys., 2015, **143**, 224301.
15 S. Enami, M. R. Hoffmann, A. Colussi, J. Phys. Chem. B, 2009, **113**, 9356.
16 Y. Fang, F. Liu, R. Emre, J. Liu, J. Phys. Chem. B, 2013, **117**, 2878.
17 G. N. Khairallah, A. T. Maccarone, H. T. Pham, T. M. Benton, T. Ly, G. da Silva, S. J. Blanksby, R. A. J. O'Hair, Angew. Chem. Int. Ed., 2015, **54**, 12947.
18 D. Scuderi, E. Bodo, B. Chiavarino, S. Fornarini, M. E. Crestoni, Chem. - Eur. J., 2016, **22**, 17239.
19 E. F. van der Eide, G.-L. Hou, S. H. M. Deng, H. Wen, P. Yang, R. M. Bullock, X.-B. Wang, Organometallics, 2013, **32**, 2084.
20 Z. B. Qin, G. L. Hou, Z. Yang, M. Valiev, X. B. Wang, J. Chem. Phys., 2016, **145**, 214310.
21 X.-B. Wang, S. R. Kass, J. Am. Chem. Soc., 2014, 136, 17332.
22 X. B. Wang, L. S. Wang, Rev. Sci. Instrum., 2008, **79**, 073108.
23 M. J. Frisch, G. W. Trucks, and H. B. Schlegel et al. Gaussian 09, Revision D.01, Gaussian, Inc., Wallingford, CT, 2009.
24 T. Yanai, D. P. Tew, N. C. Handy, Chem. Phys. Lett., 2004, **393**, 51.
25 E. Papajak, H. R. Leverentz, J. Zheng, D. G. Truhlar, J. Chem. Theory Comput., 2009, **5**, 1197.

26 G. E. Scuseria, C. L. Janssen, H. F. Schaefer, J. Chem. Phys., 1988, **89**, 7382.
27 Dhara, Ghosh, Phys. Rev. A, 1987, **35**, 442.
28 D. Jacquemin, V. Wathelet, E. A. Perpete, C. Adamo, J. Chem. Theory Comput., 2009, **5**, 2420.
29 A. E. Reed, R. B. Weinstock, F. Weinhold, J. Chem. Phys., 1985, **83**, 735.
30 X. Bao, D. A. Hrovat, W. T. Borden, X.-B. Wang, J. Am. Chem. Soc., 2013, **135**, 4291.
31 B. Chen, D. A. Hrovat, S. H. M. Deng, J. Zhang, X.-B. Wang, W. T. Borden, J. Am. Chem. Soc., 2014, **136**, 3589.
32 D. Hrovat, A. G.-L. Hou, B. Chen, X.-B. Wang, W. T. Borden, Chem. Sci., 2016, **7**, 1142.
33 Z. Yang, D. A. Hrovat, G.-L. Hou, W. T. Borden, X.-B. Wang, J. Phys. Chem. A, 2019, **123**, 3142.
34 G. Gryn'ova, D. L. Marshall, S. J. Blanksby, M. L. Coote, Nat. Chem., 2013, **5**, 474.
35 G. Gryn’ova, M. L. Coote, J. Am. Chem. Soc., 2013, **135**, 15392.
36 T. Kusamoto, S. Kume, H. Nishihara, J. Am. Chem. Soc., 2008, **130**, 13844.
37 T. Kusamoto, S. Kume, H. Nishihara, Angew. Chem. Int. Ed., 2010, **49**, 529.
38 H. Guo, Q. Peng, X.-K. Chen, Q. Gu, S. Dong, E. W. Evans, A. J. Gillett, X. Ai, M. Zhang, D. Credgington, V. Coropceanu, R. H. Friend, J.-L. Brédas, F. Li, Nat. Mater., 2019, **18**, 977.
39 S. E. Wheeler, WIREs Computational Molecular Science, 2012, **2**, 204.
40 H. Jangra, H. Zipse, J. Phys. Chem. B, 2018, **122**, 8880.
41 H. Xiao, M. P. Jedrychowski, D. K. Schweppe, E. L. Huttlin, Q. Yu, D. E. Heppner, J. Li, J. Long, E. L. Mills, J. Szpyt, Z. He, G. Du, R. Garrity, A. Reddy, L. P. Vaites, J. A. Paulo, T. Zhang, N. S. Gray, S. P. Gygi, E. T. Chouchani, Cell, 2020, **180**, 968.

PAPER

Distonic radical anion species in cysteine oxidation processes†

Zhengbo Qin,*[a] Gao-Lei Hou,[b] Zheng Yang,[b] Marat Valiev,*[c] and Xue-Bin Wang*[b]

Received 00th January 20xx,
Accepted 00th January 20xx

DOI: 10.1039/x0xx00000x

www.rsc.org/chemicalscience

Table of Contents

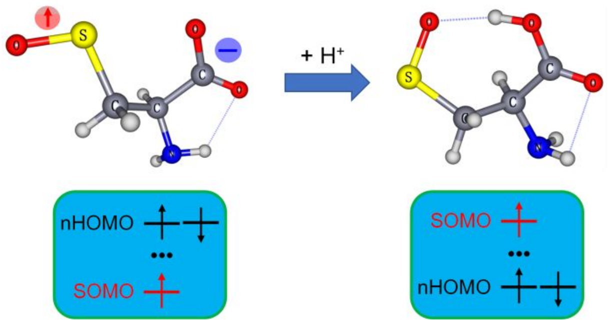

Contrary to the view that the first reversible oxidation step is associated with sulfinate species, a novel distonic radical anion •OS-$CH_2CH(NH_2)$-COO^- has been identified from direct cryo-NIPES experiments with inverted SOMO-HOMO energy order that can be restored via protonation.

---

[a] Anhui Province Key Laboratory of Optoelectric Materials Science and Technology, Anhui Normal University, Wuhu, 241000, China. E-mail: wave0403@163.com.
[b] Physical Sciences Division, Pacific Northwest National Laboratory, 902 Battelle Boulevard, P. O. Box 999, MS K8-88, Richland, Washington 99352, USA. E-mail: xuebin.wang@pnnl.gov.
[c] Environmental Molecular Sciences Laboratory, Pacific Northwest National Laboratory, P. O. Box 999, Richland, WA 99352, USA. E-mail: marat.valiev@pnnl.gov.

† Footnotes relating to the title and/or authors should appear here.

† Electronic Supplementary Information (ESI) available. See DOI: 10.1039/x0xx00000x